

# The Climate Simulated by the JMA Global Model Part 1 : Global Feature

By

**Masato SUGI\***, **Ryuichi KAWAMURA\*** and **Nobuo SATO\*\***

*\*National Research Institute for Earth Science and Disaster Prevention*

*\*\*Japan Meteorological Agency*

## **Abstract**

A 34-year simulation of the global atmospheric circulation has been performed using the Japan Meteorological Agency (JMA) global model as an atmospheric general circulation model (AGCM). The simulated climate is compared with observed climate. It is found that the JMA global model is able to simulate the present global climate reasonably well and can be used as an AGCM.

**Key Words** : model, climate, JMA, global

## **1. Introduction**

The Japan Meteorological Agency (JMA) global forecast model is used as an atmospheric general circulation model (AGCM) at the National Research Institute for Earth Science and Disaster Prevention (NIED). In the future this model is going to be coupled with the Geophysical Fluid Dynamics Laboratory (GFDL) oceanic general circulation model (OGCM) to develop a climate model for predicting the possibility of future disasters.

The JMA model used at NIED is the current operational version of the global forecast model at JMA. A description of the model is found in JMA (1993) and Sugi *et al.* (1990). The model is known to perform well as a forecast model (JMA, 1993 ; Sugi *et al.*, 1990 ; Bourke *et al.*, 1991), but the performance of the model as a GCM has not been fully investigated yet. The performance of the model as an AGCM needs to be

---

\*Atmospheric and Hydrospheric Science Division

examined before coupling it with OGCM.

In order to investigate the climate of the JMA global model, the T42/L21 (the maximum zonal wave number is 42 and the number of vertical levels is 21) GCM version of the model has been time-integrated for a period of 34 years. The observed sea surface temperature from 1955 to 1988 was used as a boundary condition during the simulation. The climate of the model is defined as a 34 year average of the monthly mean fields or seasonal mean fields of the simulation. For the verification of the simulated climate, a 10 year average of the European Centre for Medium Range Weather Forecasting (ECMWF) objective analysis for 1980-1989 is used. For precipitation, the observed climate by Jaeger (1976) is used.

In this paper, the global features of the simulated climate are described. In the second paper (Sugi *et al.* 1995), the simulated climate of tropical precipitation is presented.

## **2. Geographical Distribution**

### **2.1 Sea level pressure**

The observed and simulated climates of the monthly mean sea level pressure for the four months, January, April, July and October, are shown in **Fig. 1(a)** and **1(b)**, respectively. The seasonal change of the geographical distribution of the sea level pressure is fairly well simulated by the model. In January, however, both the simulated Aleutian low and Siberian high are stronger than the observed ones. The simulated Aleutian low is also stronger in April. In summer, the simulated Pacific subtropical high extends a little too far westward, and the ridge line is located a little north of the observed location. The simulated Atlantic subtropical high is elongated from the south-west to the north-east.

### **2.2 500 hPa height field**

The observed and simulated climates of the monthly mean 500 hPa height field and their differences are shown in **Fig. 2**. Large differences are found in the winter over the Western Hemisphere with negative maxima over the west coast of Canada and the North Atlantic and a positive maximum over the eastern part of Canada. This pattern in the difference field corresponds to the weakening of the planetary wave in the model over this region. The planetary wave ridge over the Rocky Mountains and the trough over north-eastern Canada in the model are weaker than the observed ones. This weakening of the planetary wave is commonly found in many models and referred to as "zonalization" (Boer *et al.*, 1991).

In April, a large negative difference is found in the Eastern Hemisphere, over the Sea of Okhotsk and north-eastern Europe, where the simulated planetary wave trough is deeper than the observed one.

In April, July and October, a negative difference is found over the region to the south of New Zealand. In the observed 500 hPa height field, there is a diffluence over New Zealand and a planetary wave ridge to the south of it. Such diffluence is not evident in the simulated field.

### **2.3 850 hPa wind**

The observed and simulated climates of the monthly mean 850 hPa wind are displayed in **Fig. 3**. The geographical distribution and magnitude of the 850 hPa wind are fairly well simulated by the model.

In January, however, the westerly wind over Siberia and the north-westerly wind over North America are not well simulated. In July, the monsoon southwesterly wind over the Arabian Sea is simulated very well, but the simulated monsoon flow extends too far north-eastward along the Asian continent.

### **2.4 Stream function and velocity potential at 200 hPa**

The observed and simulated climates of the stream function and velocity potential at 200 hPa are shown in **Fig. 4** and **Fig. 5**, respectively. The stream function at 200 hPa is fairly well simulated by the model. In January, zonalization over North America is noted. In July, the simulated Tibetan high and easterly jet to the south of it are a little stronger than the observed ones.

The pattern of the velocity potential is also well simulated by the model, but the magnitude of the simulated velocity potential is considerably larger than that of the observed one. The gradient of the velocity potential, and therefore, the divergent wind is stronger in the model, particularly over Africa and the central Pacific. It should be noted, however, that the analyzed divergent wind is dependent on the model used for the objective analysis. It is possible that the divergent wind in the ECMWF model used for the objective analysis may not be so strong as that in recent models.

### **2.5 Precipitation**

**Fig. 6** shows both the observed (Jaeger, 1976) and simulated climates of the monthly mean precipitation for January and July. The overall geographical distribution of precipitation is well simulated. In January, however, excessive precipitation is simulated along the storm tracks in the North Pacific and North Atlantic. In contrast, the intensity of the simulated precipitation in July along the circumpolar storm track in the Southern

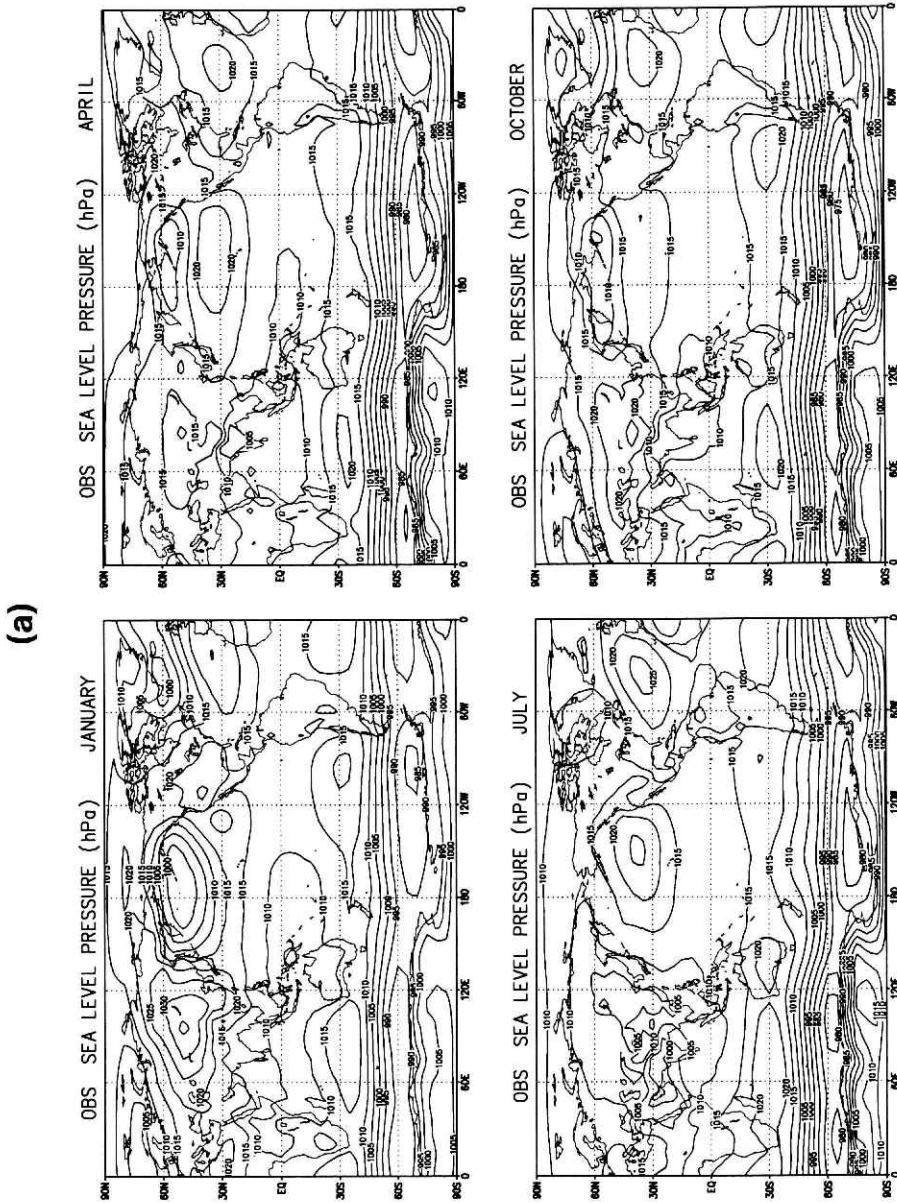
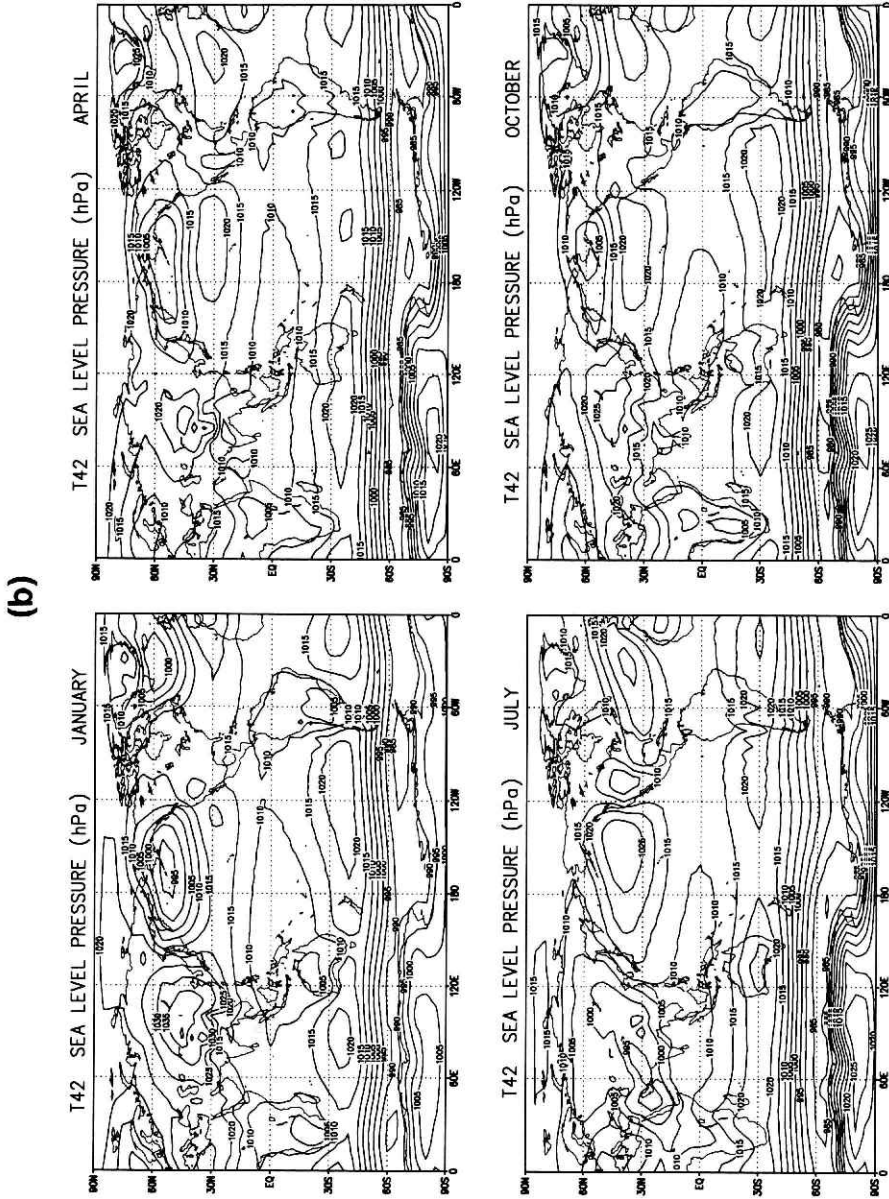
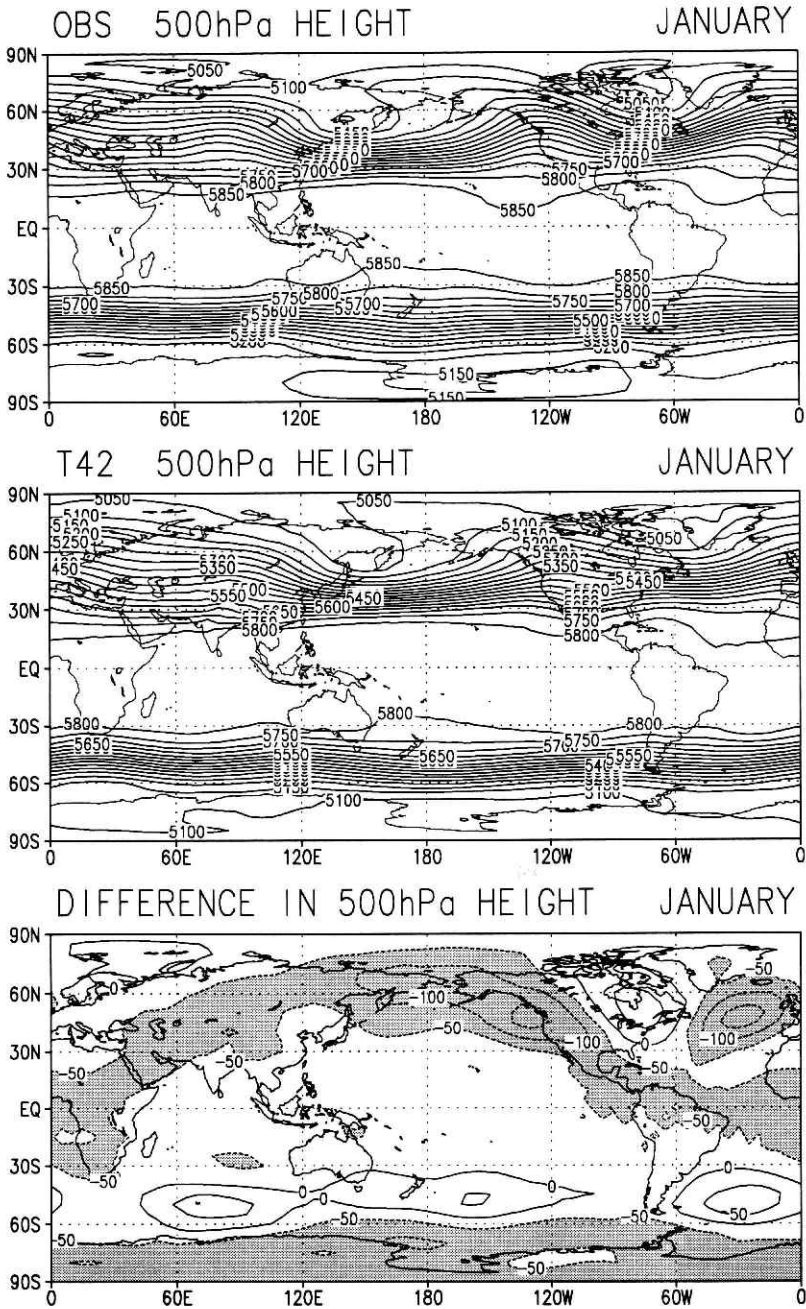


Fig. 1-(a) Observed mean sea level pressures for January, April, July, and October. Contour interval is 5 hPa.



**Fig. 1-(b)** Simulated mean sea level pressures for January, April, July and October. Contour interval is 5 hPa.

(a)



**Fig. 2-(a)** Observed (top) and simulated (middle) 500 hPa height fields and their differences (simulated minus observed, bottom) for January. Contour interval is 50 m.

(b)

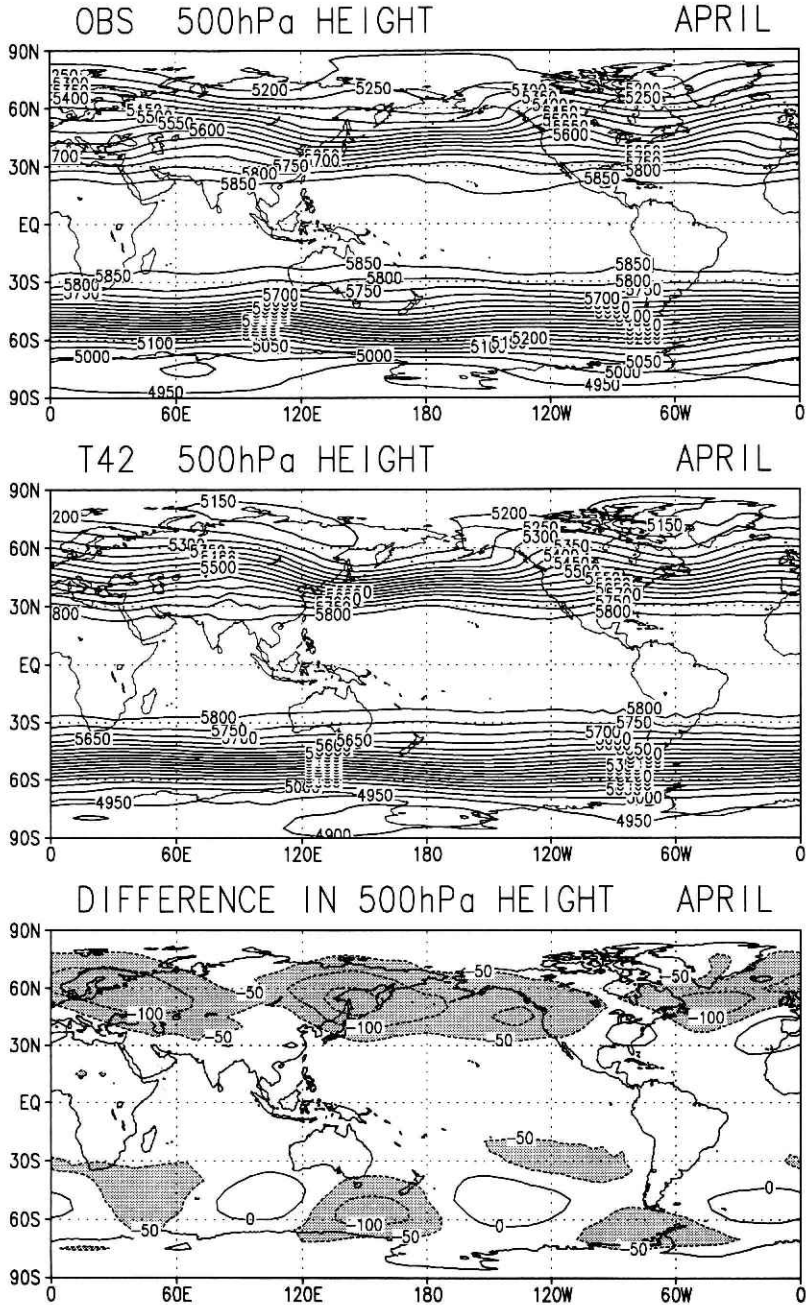


**Fig. 2-(b)** Observed (top) and simulated (middle) 500 hPa height fields and their differences (simulated minus observed, bottom) for April. Contour interval is 50 m.

(c)

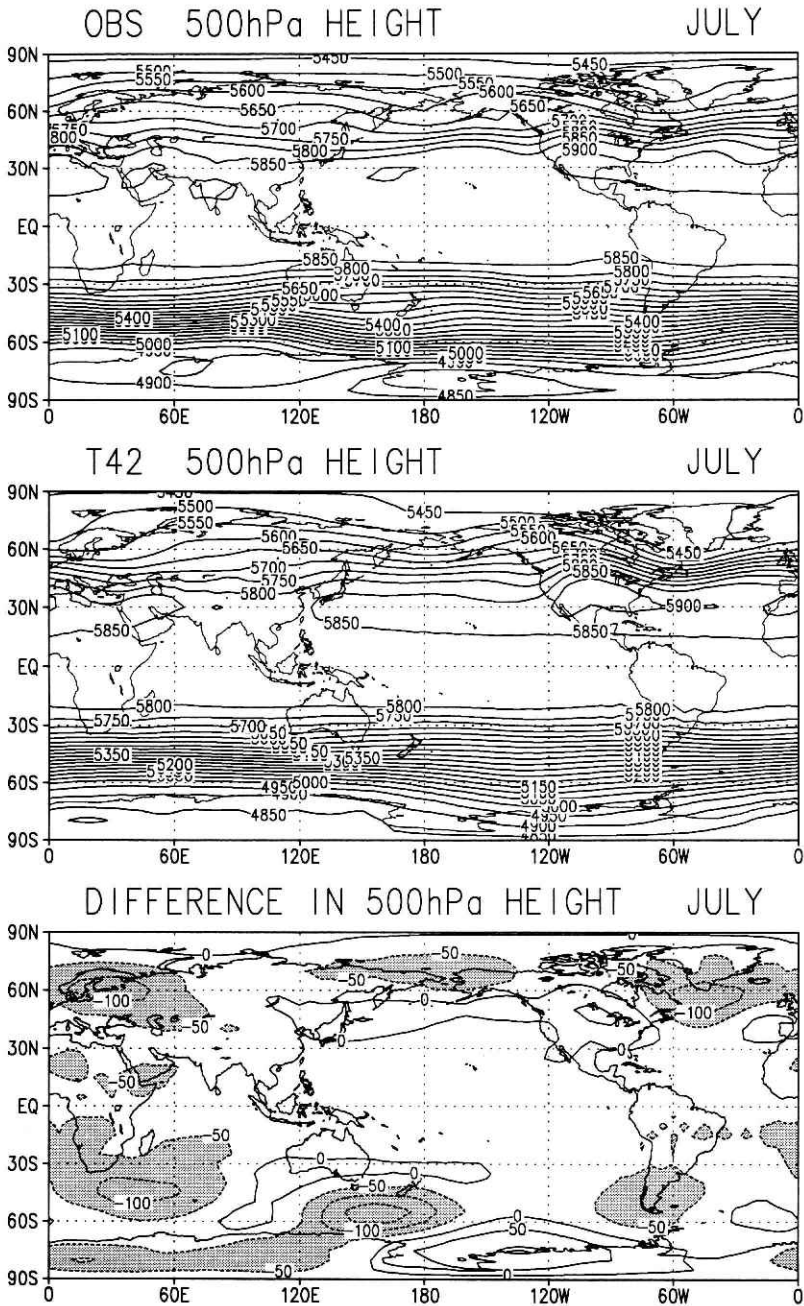
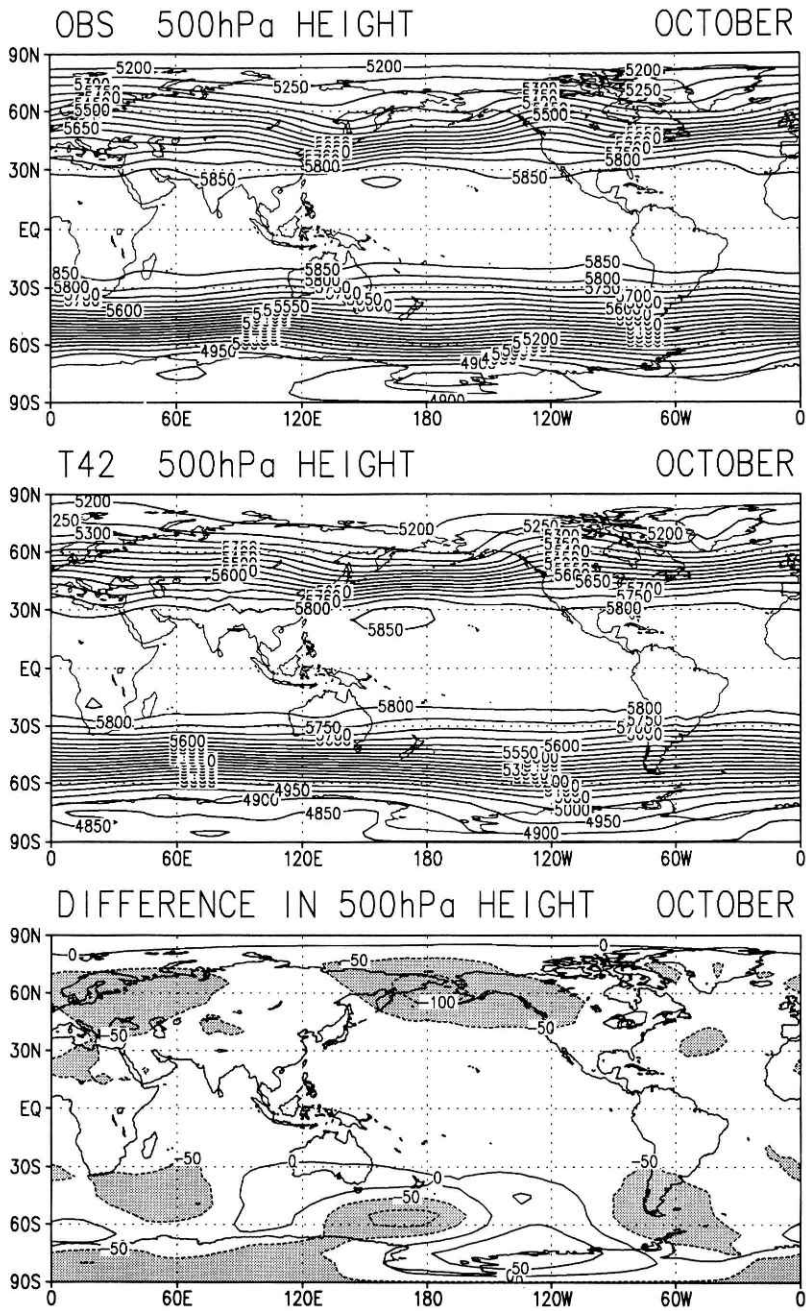


Fig. 2-(c) Observed (top) and simulated (middle) 500 hPa height fields and their differences (simulated minus observed, bottom) for July. Contour interval is 50 m.

(d)



**Fig. 2-(d)** Observed (top) and simulated (middle) 500 hPa height fields and their differences (simulated minus observed, bottom) for October. Contour interval is 50 m.

(a)

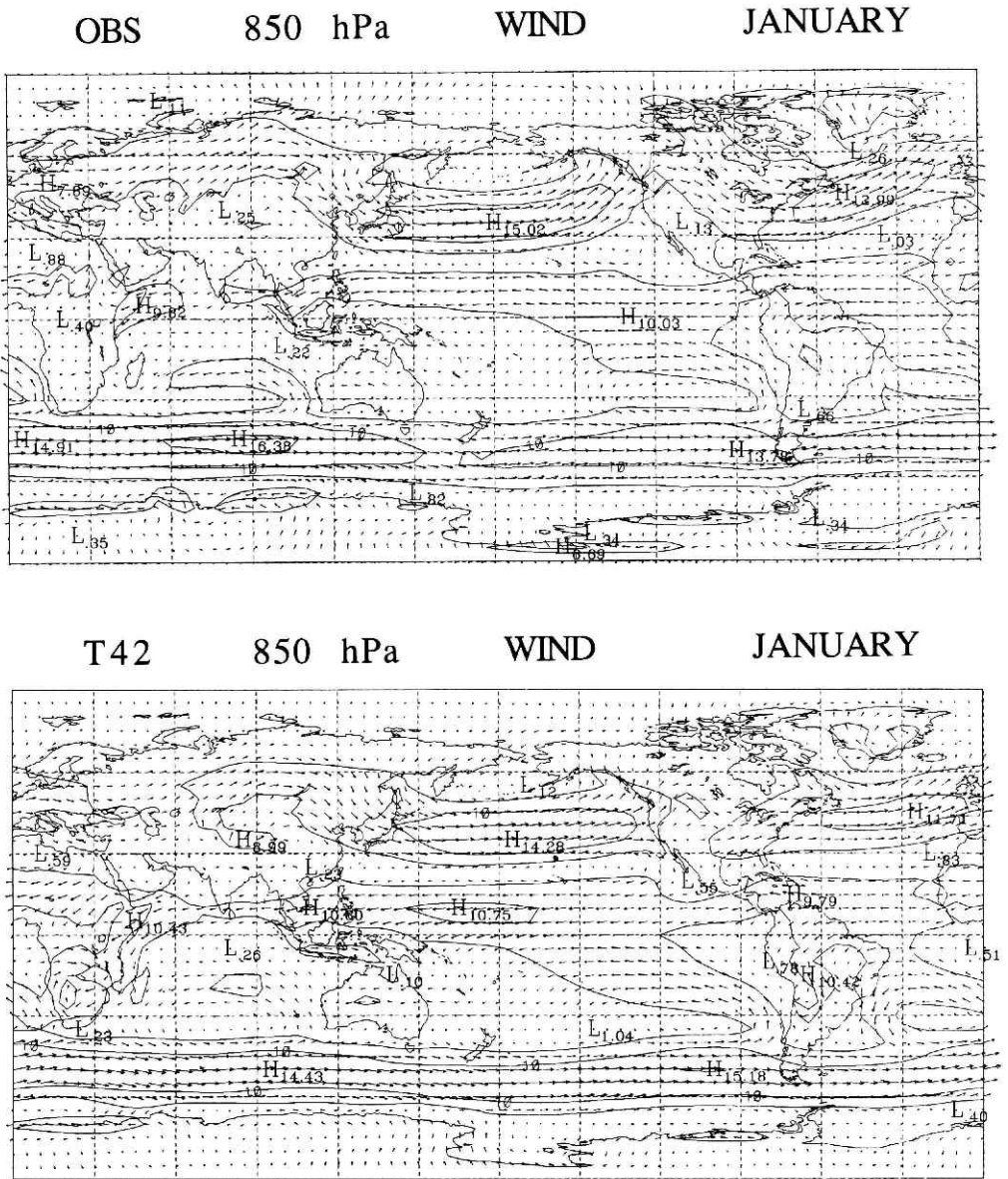
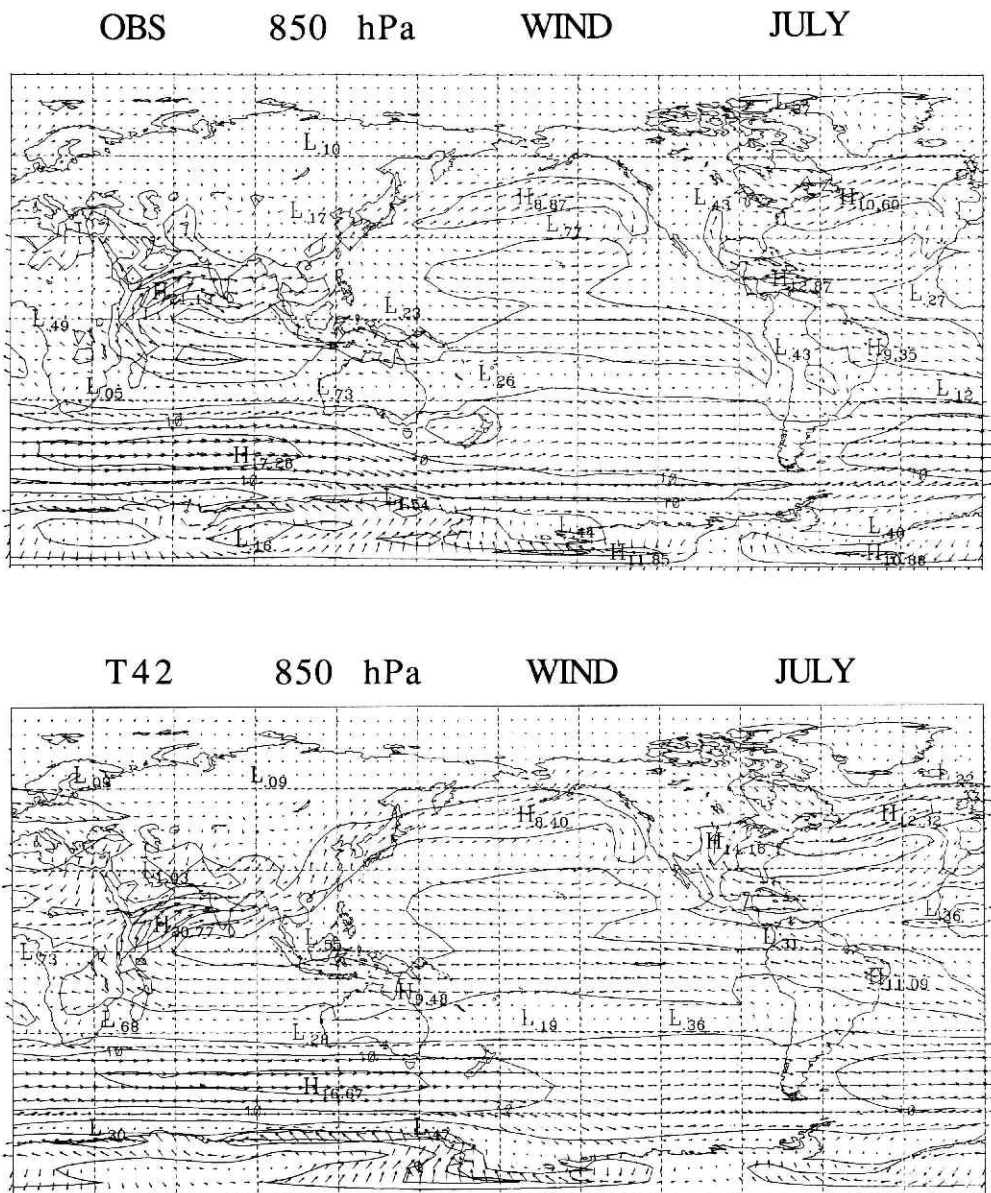


Fig. 3-(a) Observed (top) and simulated (bottom) 850 hPa wind for January. Contours show wind speed. Contour interval is 5 m/sec.

(b)



**Fig. 3-(b)** Observed (top) and simulated (bottom) 850 hPa wind for July. Contours show wind speed. Contour interval is 5 m/sec.

(a)

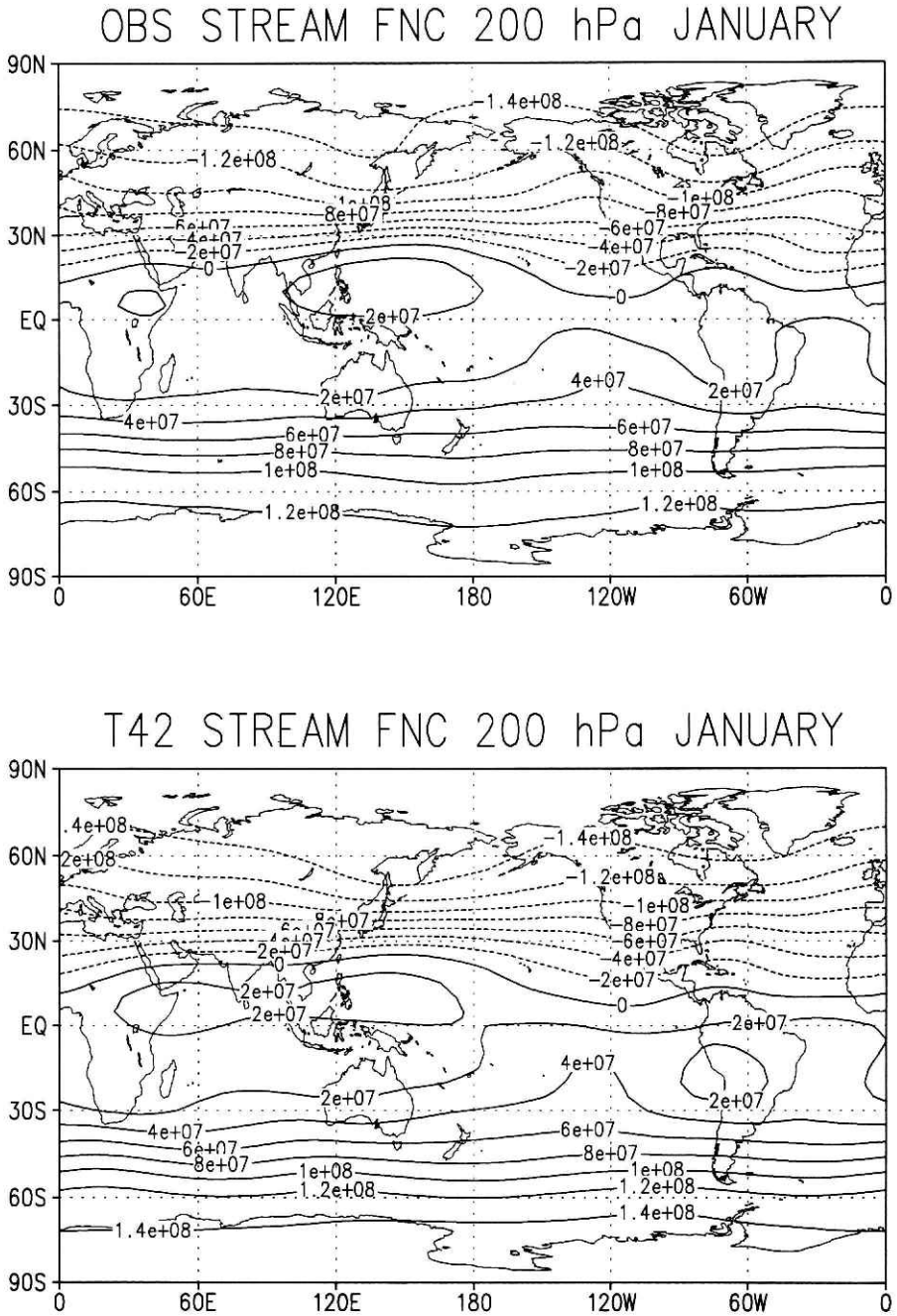


Fig. 4-(a) Observed (top) and simulated (bottom) stream function at 200 hPa for January.

(b)

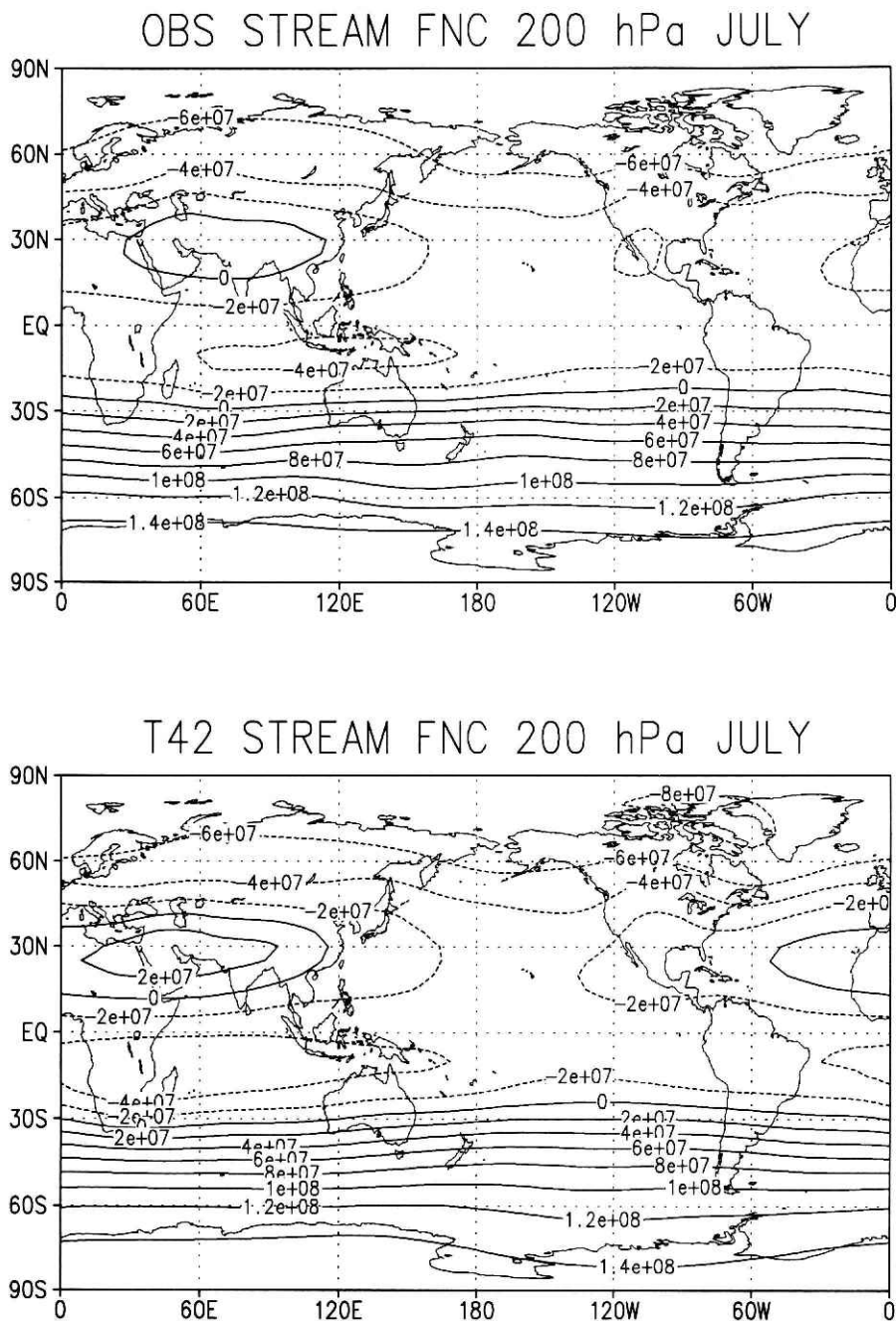


Fig. 4-(b) Observed (top) and simulated (bottom) stream function at 200 hPa for July.

(a)

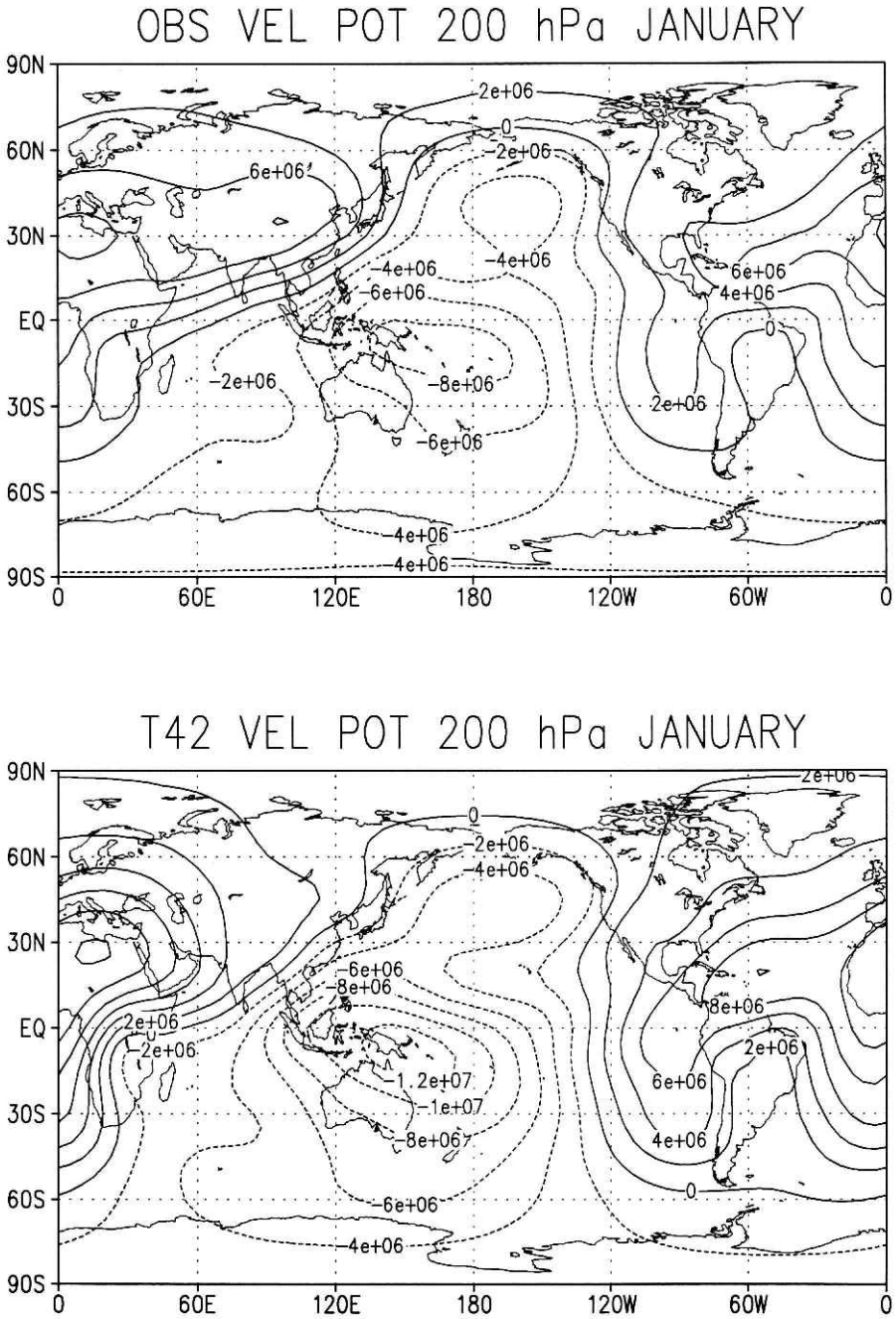


Fig. 5-(a) Observed (top) and simulated (bottom) velocity potential at 200 hPa for January.

(b)

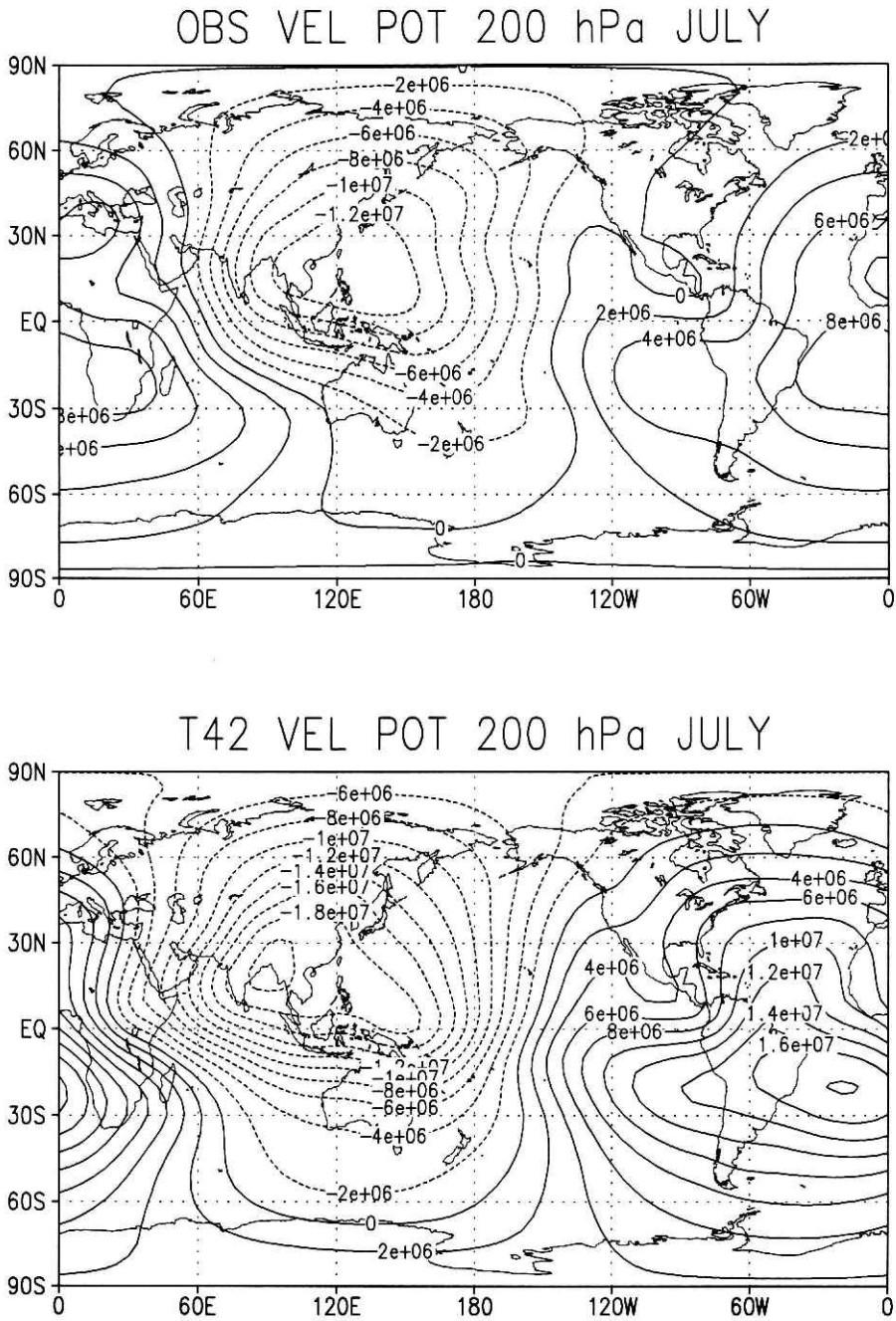
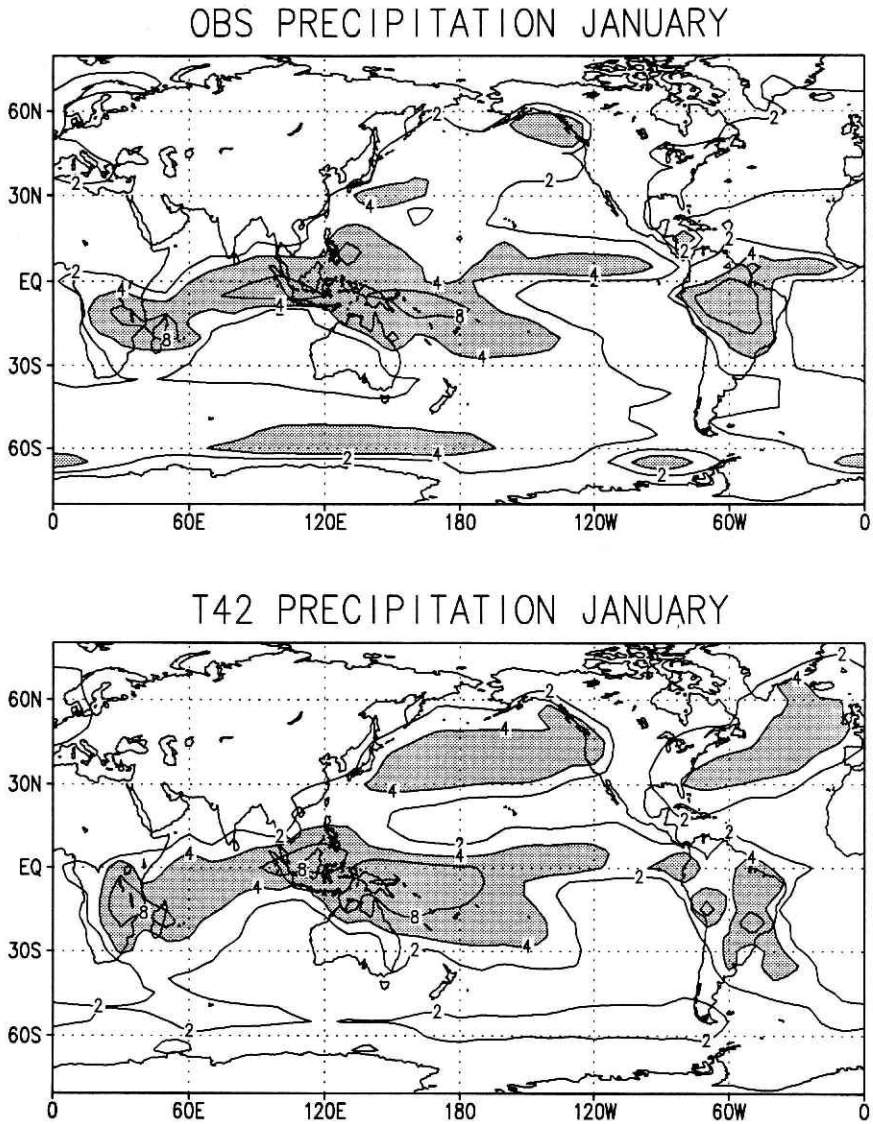


Fig. 5-(b) Observed (top) and simulated (bottom) velocity potential at 200 hPa for July.

(a)



**Fig. 6-(a)** Observed (Jaeger, 1976, top) and simulated (bottom) precipitation for January. Contours are 1, 2, 4, 8, ... mm/day. Areas 4 mm/day are shaded.

(b)

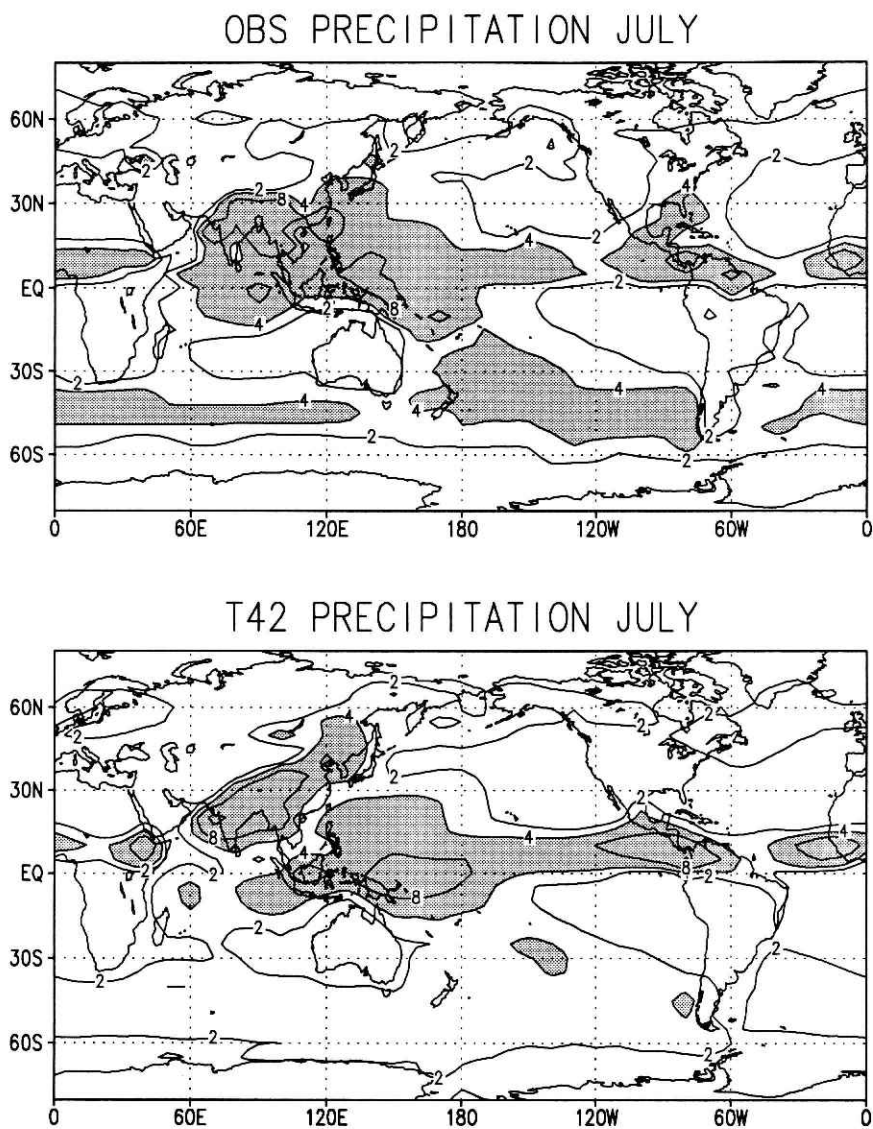


**Fig. 6-(b)** Observed (Jaeger, 1976, top) and simulated (bottom) precipitation for July. Contours are 1, 2, 4, 8, ... mm/day. Areas 4 mm/day are shaded.

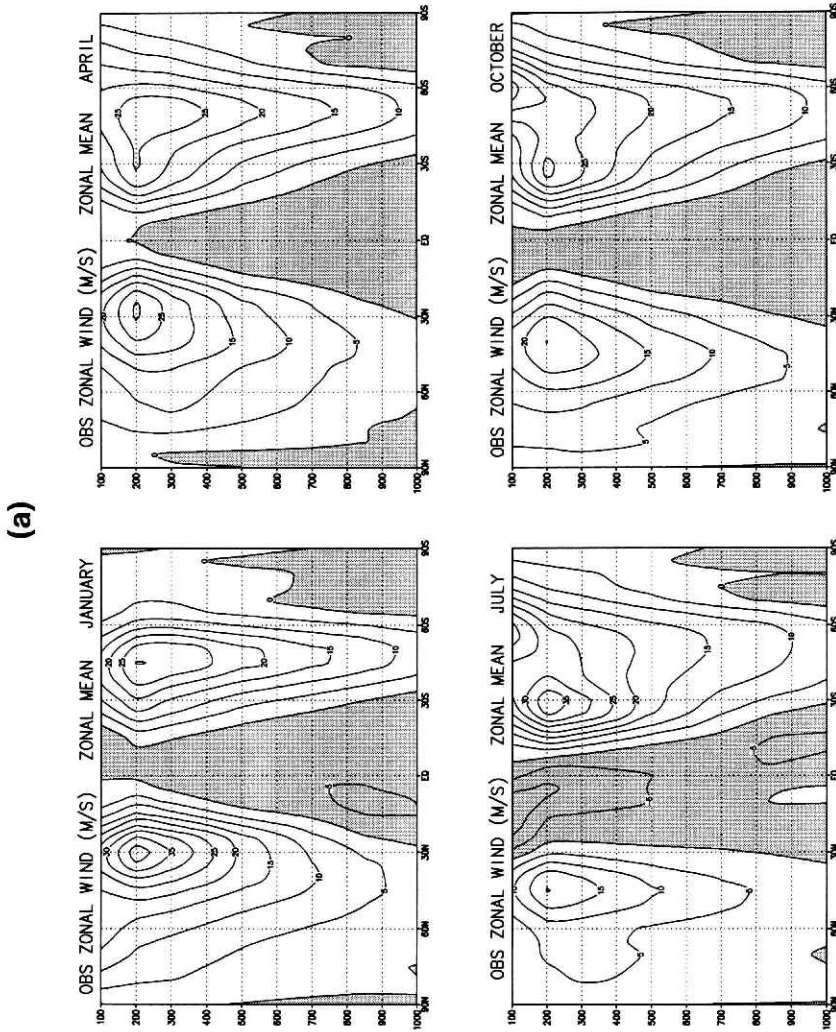
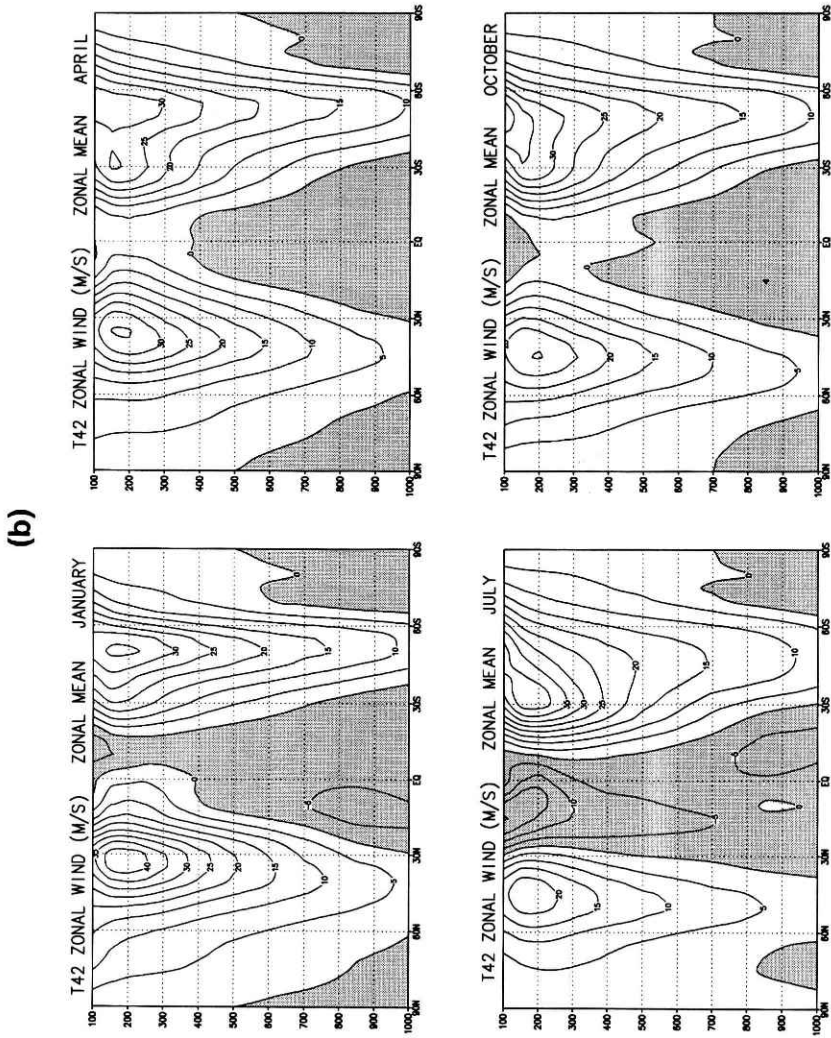
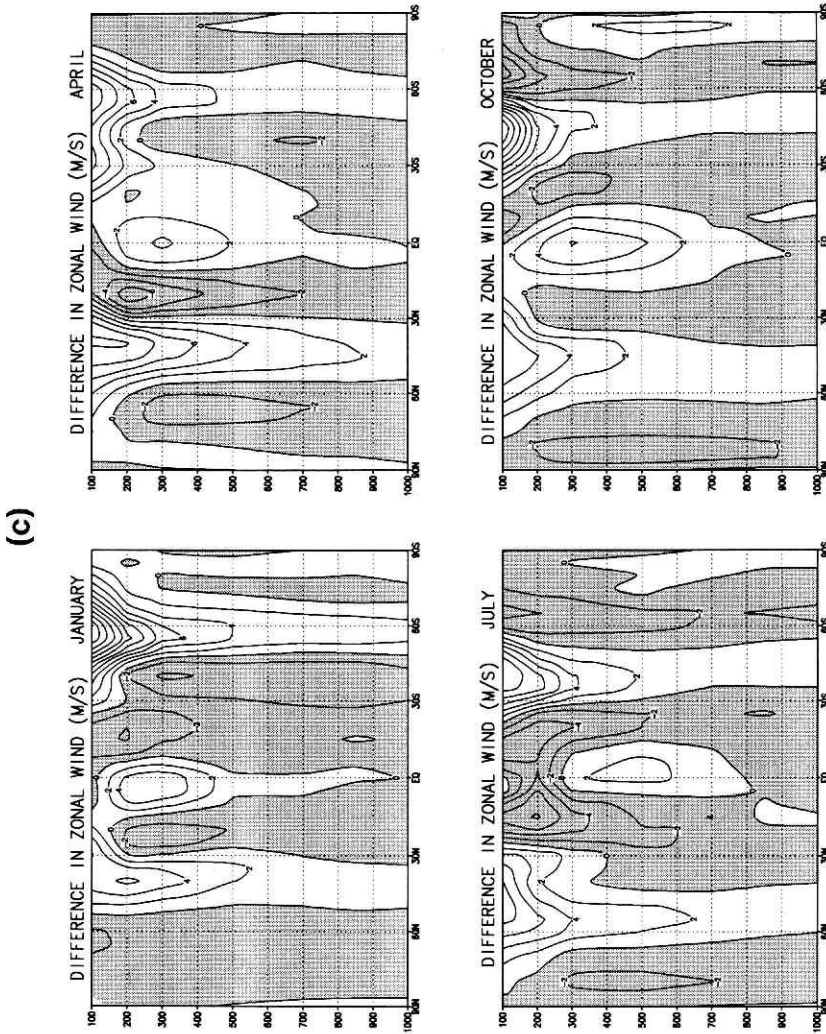


Fig. 7-(a) Observed zonal mean zonal wind for January, April, July and October. Contour intervals are 5 m/sec.



**Fig. 7-(b)** Observed zonal mean zonal wind for January, April, July and October. Contour intervals are 5 m/sec.



**Fig. 7-(c)** Difference between the observed and simulated zonal mean zonal wind (simulated minus observed). Contour intervals are 2 m/sec.

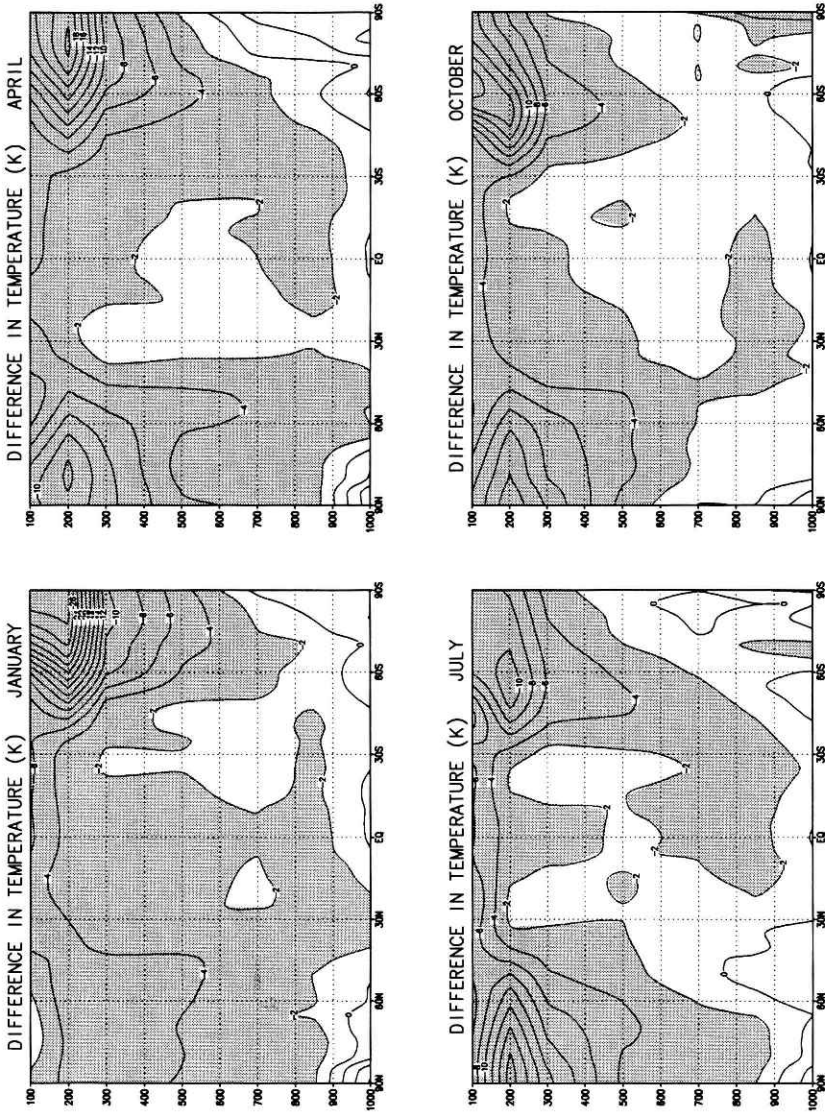


**Fig. 8** Difference between the observed and simulated zonal mean temperatures (simulated minus observed). Contour interval is 2°K. Areas below  $-2^{\circ}\text{K}$  are shaded.

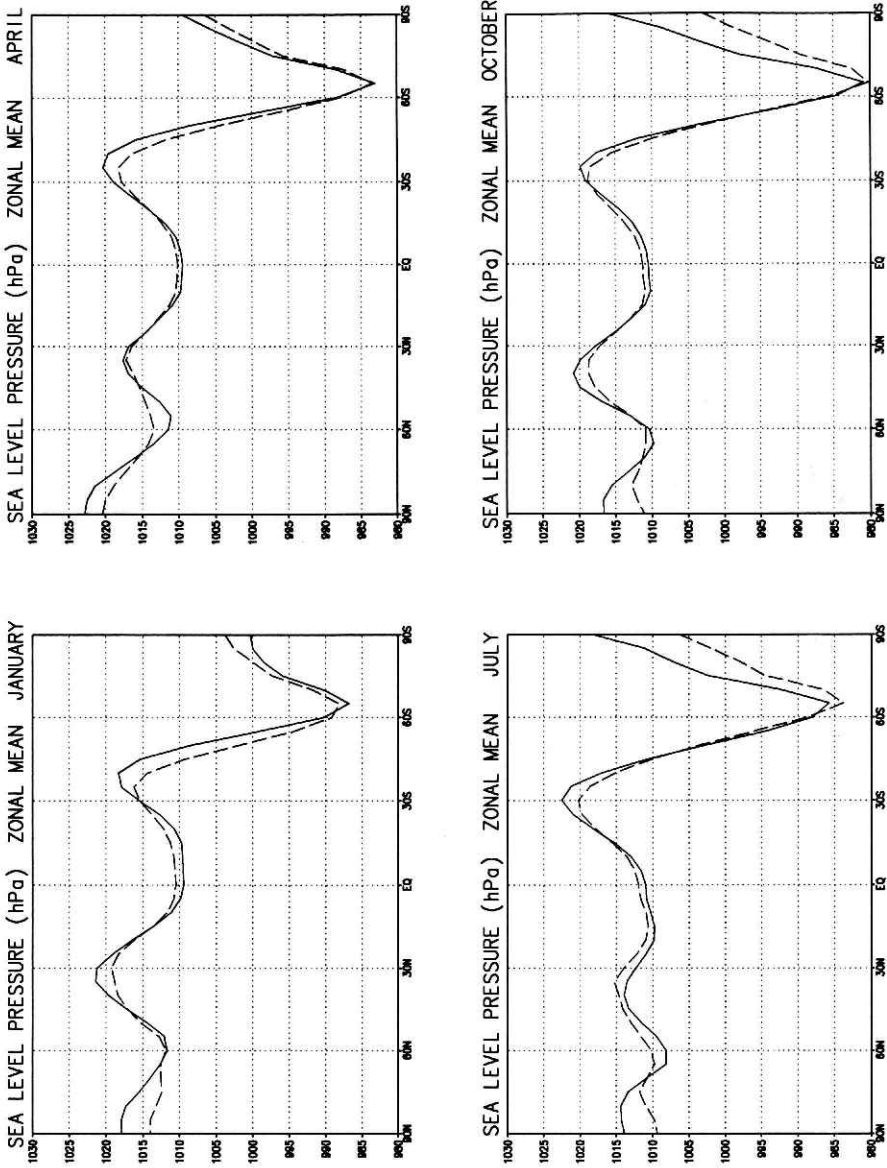


Fig. 9 Observed (dashed lines) and simulated (solid lines) zonal mean sea level pressures.

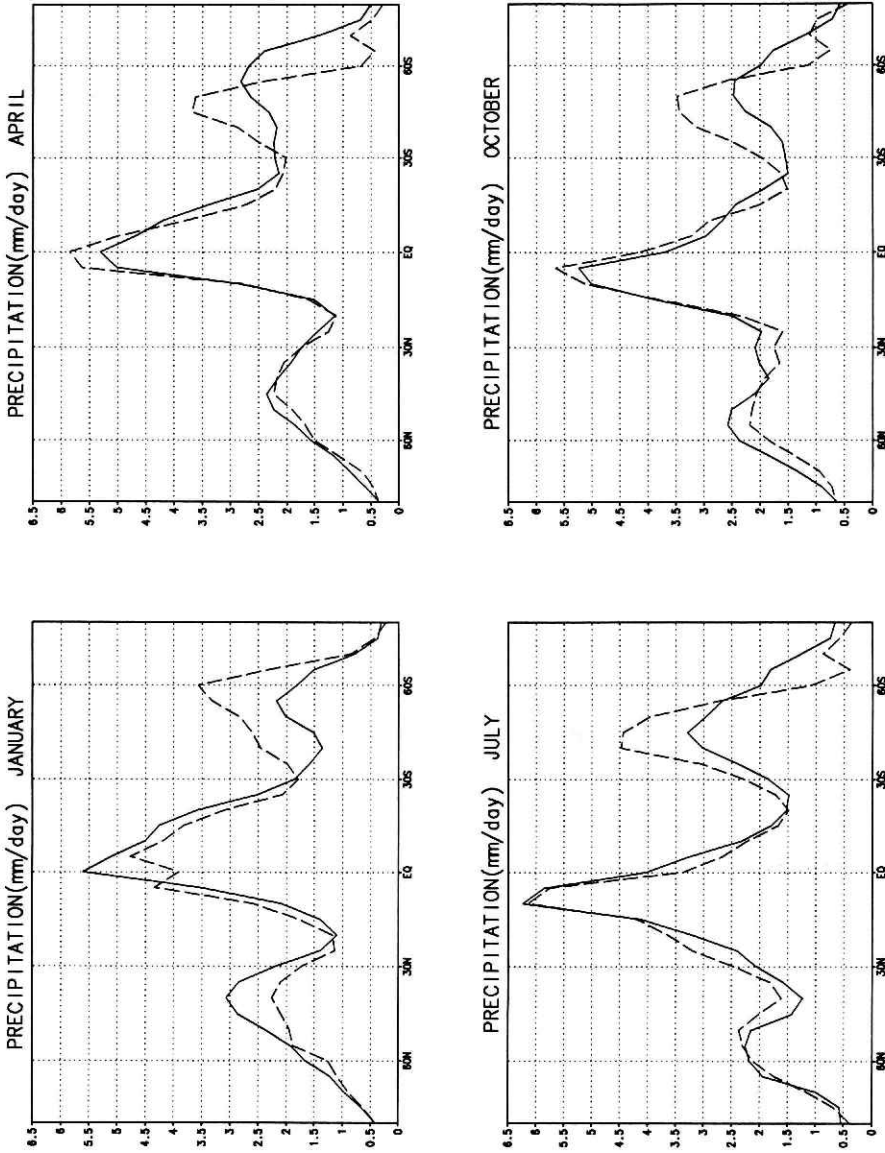


Fig. 10 Observed (dashed lines) and simulated (solid lines) zonal mean precipitation.

Hemisphere is less than of the observed. The simulation of the tropical precipitation is described further in the second paper (Sugi *et al.* 1995).

### **3. Zonal mean fields**

#### **3.1 Zonal wind**

The latitude–height sections of the zonally averaged zonal wind are shown in **Fig. 7**. The observed and simulated climates are shown in **Fig. 7(a)** and **7(b)**, respectively, and the difference between the two is shown in **Fig. 7(c)**. The intensity of simulated subtropical jet streams (wind maximum near 200hPa) is larger than that of the observed one. The simulated tropical easterly jet in July is also stronger than the observed one. In the observed field of July, a jet core around 30°S and a double jet structure in the mid-troposphere are evident, but such structures are not clear in the corresponding simulated field.

The difference between the observed and simulated zonal winds is generally small in the troposphere, but very large in the stratosphere. The large errors of zonal wind in the stratosphere correspond to the large temperature errors there.

#### **3.2 Temperature**

The latitude–height sections of the zonally averaged difference between the observed and simulated temperatures are shown in **Fig. 8**. The simulated temperature is lower than the observed temperature almost everywhere. In the troposphere, the simulated temperature is lower than the observed one by less than two degrees. At high latitudes of the stratosphere, however, the simulated temperature is significantly lower than the observed one.

#### **3.3 Sea level pressure**

The observed and simulated zonal mean sea level pressures are shown in **Fig. 9**. The latitudinal distribution of the sea level pressure is fairly well simulated by the model, including the deep circumpolar trough in the Southern Hemisphere.

#### **3.4 Precipitation**

The observed (Jaeger, 1976) and simulated zonal mean precipitation are shown in **Fig. 10**. The latitudinal distribution of the precipitation is well simulated except for the poleward area of 30°S. The model fails to simulate the large middle-latitude maximum in the observation. On the other hand, the simulated precipitation in the middle-latitude of the Northern Hemisphere is larger than the observed one.

#### 4. Summary and conclusions

The JMA global model has been used operationally for medium range weather forecasting and it is known to have good performance as a forecast model (JMA, 1993; Sugi *et al.*, 1990; Bourke *et al.*, 1991). The 34 year time integration of a GCM version of the JMA global model has revealed that the model is able to simulate global climate reasonably well in the troposphere. Systematic errors such as a cool bias and zonalization which are common in many GCMs (Boer *et al.*, 1991), are also found in the JMA global model. In addition to these systematic errors, we have found some differences between the simulated and observed climates, but the magnitude of the differences is generally small and comparable to that of many other GCMs (Boer *et al.*, 1991). Therefore, we may conclude that the performance of the JMA global model as a GCM is comparable or superior to many other GCMs.

On the other hand, the simulated climate of the JMA global model in the stratosphere is not so good as in the troposphere. This is mainly because the top level of the model where the variables are defined is too low and the vertical resolution is coarse in the stratosphere. Thus, the stratosphere is not fully represented in the model. This may be one of the major deficiencies of the JMA global model as a GCM.

#### 5. Acknowledgments

This study is conducted as a part of a special research project "A study of disaster prediction in global hydrological processes" at the National Research Institute for Earth Science and Disaster Prevention (NIED). The 34 year integration of the JMA global model was carried out using a CRAY-YMP2E at NIED. The authors would like to express their sincere thanks to the Japan Meteorological Agency for providing us with the JMA global forecast model and allowing us to use it for our study.

#### References

- 1) Boer, G.J., K. Arpe, M. Blackburn, M. Deque, W.L. Gates, T.L. Hart, H. le Treut, E. Roeckner, D. A. Sheinin, I. Simmonds, R.N.B. Smith, T. Tokioka, R.T. Wetherald and D. Williamson (1991): An Intercomparison of the Climates Simulated by 14 Atmospheric General Circulation Models, WMO/TD-No. 425.
- 2) Bourke, W., P. Mullenmeister, K. Arpe, D. Baumhefner, P. Caplan, J.L. Kinter, S.F. Milton, W.F. Stern and M. Sugi (1991): Systematic Errors in Extended Range Predictions, WMO/TD-No. 444.
- 3) Jaeger, L. (1976): Monatskarten des Niederschlags für die ganze Erde, Berichte Deutsches Wetterdienst, Nr. 139, Offenbach, 38pp.
- 4) JMA (1993): Outline of Operational Numerical Weather Prediction at Japan Meteorological Agency, Appendix to Progress Report on Numerical Weather Prediction, JMA, 128pp.

- 5) Sugi, M., K. Kuma, K. Tada, K. Tamiya, N. Hasegawa, T. Iwasaki, S. Yamada and T. Kitade (1990): Description and performance of the JMA Operational Global Spectral Model (JMA-GSM88), *Geophys. Mag.*, **43**-3, 105~130.
- 6) Sugi, M., Nair, R. D., Sato, N.(1995): The Climate Simulated by the JMA Global Model, part 2: Tropical Precipitation, Report of the Nat. Res. Inst. for Earth Science and Disaster Prevention, No. **54**, 181~197.

(Accepted : 17 August, 1994)

## 気象庁全球モデルの気候特性(1)：全球の特性

杉 正人\*・川村隆一\*・佐藤信夫\*\*

\*防災科学技術研究所 気圏・水圏地球科学技術研究部

\*\*気象庁 予報部 数値予報課

### 要 旨

気象庁全球モデルを大気大循環モデルとして用いて、全球大気大循環の34年間の変化のシミュレーションを行った。シミュレートされたモデルの気候特性を観測と比較した。気象庁全球モデルは現在の地球の気候状態を大体良好に再現しており、大気大循環モデルとして使用できることが確認された。

キーワード：モデル (model), 気候 (climate), 気象庁 (JMA), 全球 (global)